JACS
JOURNAL OF THE AMERICAN CHEMICAL SOCIETY
Article
pubs.acs.org/JACS

# Synthesis and Photophysics of Fully π-Conjugated Heterobis-Functionalized Polymeric Molecular Wires via Suzuki Chain-Growth Polymerization

Einat Elmalem,[†] Frank Biedermann,[†] Kerr Johnson,[‡] Richard H. Friend,[‡] and Wilhelm T. S. Huck*[,†,§]

[†]Melville Laboratory for Polymer Synthesis, Department of Chemistry, University of Cambridge, Cambridge, CB2 1EW, United Kingdom

[‡]Cavendish Laboratory, Department of Physics, University of Cambridge, JJ Thomson Avenue, Cambridge, CB3 0HE, United Kingdom

[§]Institute for Molecules and Materials, Radboud University Nijmegen, Heyendaalseweg, 135 6525 AJ Nijmegen, The Netherlands

Supporting Information

**ABSTRACT:** We present a fast and efficient *in situ* synthetic approach to obtain fully π-conjugated polymers with degrees of polymerization up to 23 and near quantitative (>95%) heterobis-functionalization. The synthesis relies on the key advantages of controlled Suzuki chain-growth polymerization: control over molecular weight, narrow polydispersity, and ability to define polymer end groups. The first end group is introduced through the initiator metal complex $t$Bu$_3$PPd(X)Br, while the second end group is added by quenching of the chain-growth polymerization with the desired boronic esters. In all cases, polymers obtained at 50% conversion showed excellent end group fidelity and high purity following a simple workup procedure, as determined by MALDI-TOF, GPC, and $^1$H and 2D NMR. End group functionalization altered the optoelectronic properties of the bridge polymer. Building on a common fluorene backbone, and guided by DFT calculations, we introduced donor and acceptor end groups to create polymeric molecular wires exhibiting charge transfer and energy transfer as characterized by fluorescence, absorption, and transient absorption spectroscopy as well as by fluorescence lifetime measurements.

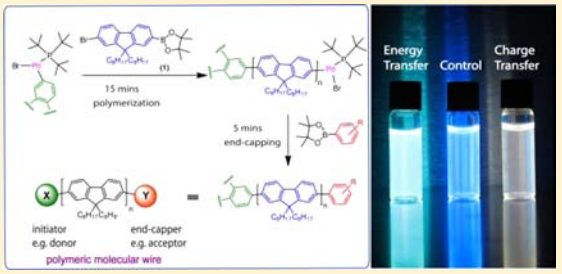


## INTRODUCTION

Conventionally, conjugated polymers are synthesized via a step-growth condensation mechanism, which typically results in poor control over crucial properties, such as kinetics, molecular weight (MW), polydispersity (PDI), and end groups.[1] The latter are especially important as the end groups not only strongly influence charge carrier properties of the polymer but also determine the photophysical and photochemical properties of the polymer backbone. For example, bromine end groups can induce intersystem crossing, which can significantly reduce the photoluminescence (PL) and adversely influence photochemical stability.[2] Recent developments in the synthetic field have enabled controlled polymerizations of conjugated polymers[3,4] with relatively narrow PDI and controlled MW.[5,6] For example, Ni-catalyzed Kumada chain-growth polymerization has been used in the synthesis of polythiophenes,[4,7−12] polyphenylenes,[13] and polyfluorenes.[14] *In situ* end group functionalization was shown for the GRIM method,[15,16] however it remains a challenge to ensure end group fidelity and heterobis end functionalization. Alternatively, Suzuki chain-growth polymerization has been recently developed to synthesize p-type homopolymers of polyfluorenes,[17−19] polyphenylenes,[20] and polythiophenes[21] as well as the n-type copolymer poly(fluorene-benzothiadiazole).[22]

Here we exploit a key feature of a chain-growth over a step-growth mechanism: The ability to independently introduce two different functional end groups (X and Y) on either side of the conjugated polymer in a facile way. While asymmetric end groups have been routinely demonstrated for 'controlled' or 'living' polymerization of nonconjugated polymers, this is the first report, despite many efforts,[23−26] where near quantitative *in situ* heterobis end group functionalization has been achieved in fully π-conjugated polymers. Figure 1a shows the general strategy which was used in this study to control the end groups via the Pd-initiator and end-capping reactions (Figure 1b,c). The first end group is introduced through a series of novel initiator metal complexes $t$Bu$_3$PPd(X)Br, while the second end group is added by quenching of the chain-growth polymerization with a monoboronic ester. As shown in Figure 1, we have chosen a range of aromatic molecules to be incorporated at the initiator side and various electron-donating or -withdrawing groups (EDG or EWG) for the quenching step. In this way, we can vary the electronic nature of both end groups such that we obtain polymeric molecular wires (PMW) exhibiting either charge transfer (CT) or energy transfer (ET), as

**Received:** August 17, 2012
**Published:** September 28, 2012

   dx.doi.org/10.1021/ja3080677 | J. Am. Chem. Soc. 2012, 134, 17769−17777

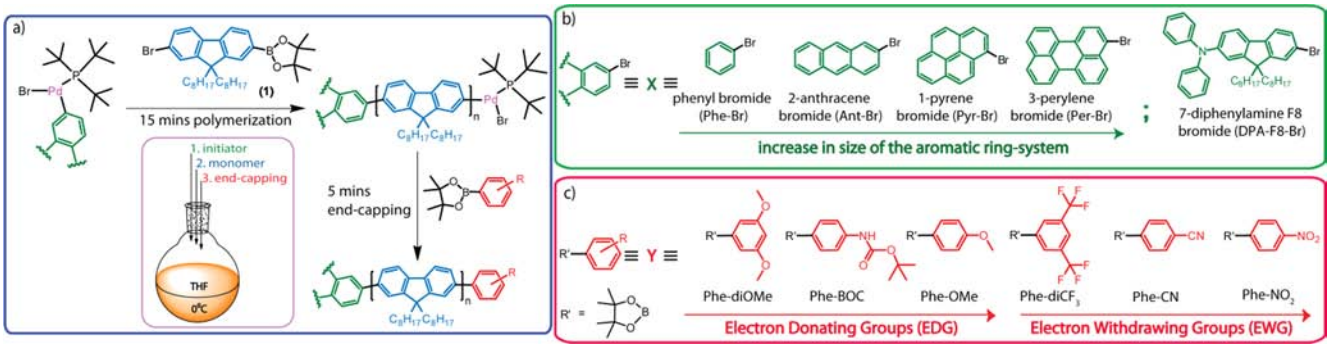


**Figure 1.** (a) General one step synthesis route which was employed in order to synthesize a variety of PMW via a Suzuki chain-growth polymerization mechanism. (b) Different aryl-bromo moieties (X) which were used for the initiator complex synthesis. (c) Different aryl-boronic-ester moieties (Y) which were used in order to quench the polymerization.

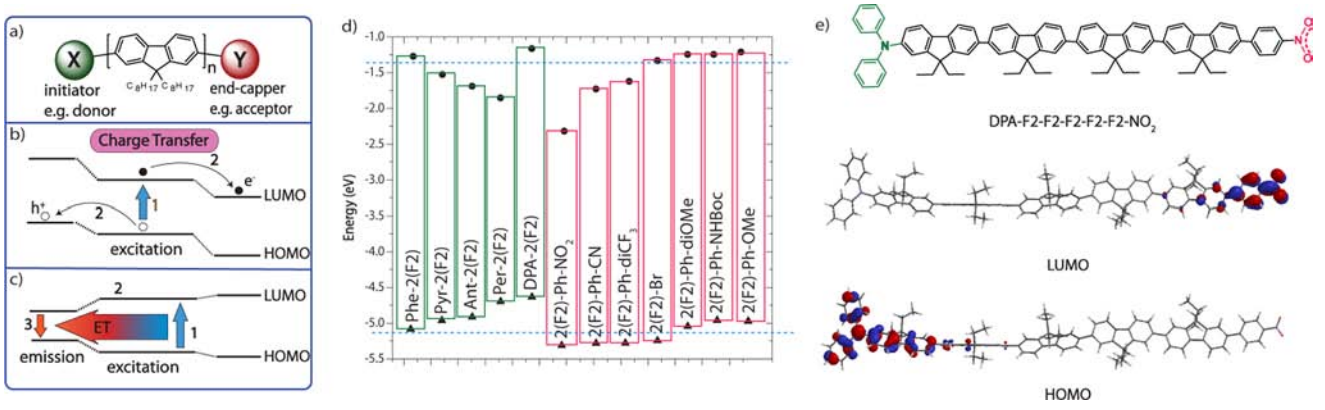


**Figure 2.** (a) Schematic depiction of the general polymeric molecular wire X−pF8−Y structure. HOMO and LUMO energy level alignment, which results in either (b) CT or (c) ET. d) DFT prediction (B3LYP/6-31G*) of the HOMO and LUMO energy levels for the polymer end groups, ranging from poor to good donors (green: from left to right) and acceptors (red: from right to left), where two units of fluorene with ethyl side-chains are coupled to the end group. The dashed blue lines represent the calculated HOMO/LUMO energy levels of four repeating units of F8. (e) Representative HOMO and LUMO orbitals of DPA−$(F2)_5$−$NO_2$, suggesting that both frontier orbitals are fully spatially separated in this particular system. For more details see Figure S1.

explained below. DFT calculations were used to guide the choice of different end groups which have suitable energy levels to interact electronically with the oligofluorene bridge.

The composition and the design of well-defined molecular wires have been given considerable attention,[27−31] and great efforts have been directed toward the synthesis of classic donor−acceptor molecular systems in order to produce long-lived charge-separated states.[32−34] Various oligomeric molecular wire systems based on porphyrins,[30,35−39] oligoacetylenes, oligophenylenes,[40,41] oligothiophenes,[37] oligofluorenes,[41,42] and oligophenylenevinylenes[43] were synthesized in solution or from surfaces.[34,44,45] While the electron- and energy-transfer mechanisms of these oligomers are well understood,[28,46−48] their synthesis requires challenging, prolonged, and stepwise synthetic procedures.[28] Furthermore, as the available synthetic methods to generate molecular wires are quite limited, most of the reported studies focus either on wires with similar end groups (i.e., limited to ET process only)[49,50] or wires with short bridges ($n < 5$), which in most cases act as charge carrier hopping sites or spacers with some through-bond coupling influence on CT/ET.[51−53] We believe that a controlled synthesis of conjugated polymers would overcome these synthetic challenges and allow for the synthesis of longer molecular wires in significantly shorter time. As well as their use in fundamental CT and ET studies, these polymeric molecular wires can act as functional molecules with the central chain chromophores absorbing and the resultant excitations undergoing CT/ET to the functional end groups. The optoelectronic properties of the PMW were characterized by fluorescence, absorption, and transient absorption spectroscopy as well as by fluorescence lifetime measurements. Additionally, we show that for specific push−pull PMW, there are significant changes in the emission spectra when the solvent environment changes from apolar to Lewis-donating solvents.

## RESULTS AND DISCUSSION

**General Considerations for Polymer Design and DFT Calculations.** In order to estimate the positioning of the HOMO/LUMO energy levels as a function of the X and Y end groups and to guide the choice of donor (D) and acceptor (A) moieties, DFT calculation using the hybrid B3LYP exchange−correlation functional and split valence 6-31G* basis set were carried out (see SI for details). By varying the nature of the end groups, the energy levels can be positioned such that they favor CT and ET, as can be seen in Figure 2a−c. In addition to the energy cascade requirements, the separation of the frontier orbitals is essential. CT states would form in molecular wires with a strong donor on one end and a strong acceptor on the other, such that both the HOMO and LUMO are spatially separated. However efficient ET will be observed when both the HOMO and LUMO are located on the same end group. Figure 2d shows HOMO/LUMO energy levels for a series of


dx.doi.org/10.1021/ja3080677 | J. Am. Chem. Soc. 2012, 134, 17769−17777

end groups obtained by DFT calculations on 'half wires' in order to simplify the calculations. The trends observed are consistent with calculations on 'full wires' with four fluorene monomers (Table 1). From the calculations it can be predicted

**Table 1. DFT Calculations for D−$(F2)_4$−A Oligomers**

| polymer D−$(F2)_4$−A | $E_{HOMO}$[a] (eV) | $E_{LUMO}$[a] (eV) |
|---|---|---|
| Phe−$(F2)_4$−Phe−OMe | −3.05 | −0.897 |
| Phe−$(F2)_4$−Phe−$NO_2$ | −3.12 | −1.45 |
| Pyr−$(F2)_4$−Phe−OMe | −3.04 | −0.97 |
| Pyr−$(F2)_4$−Phe−CN | −3.08 | −1.09 |
| Pyr-$(F2)_4$−Phe−$NO_2$ | −3.08 | −1.45 |
| Per−$(F2)_4$−Phe−OMe | −2.92 | −1.15 |
| Per−$(F2)_4$−Phe−$NO_2$ | −2.94 | −1.45 |
| DPA−$(F2)_4$−Phe−OMe | −2.87 | −0.86 |
| DPA−$(F2)_4$−Phe−$NO_2$ | −2.89 | −1.45 |

[a]Geometry optimized at B3LYP/6-31G* level of theory. See Figure S1 for renderings of the HOMO and LUMO orbitals.

that the strength of the donor group increases as: phenyl ≤ pyrene < perylene < DPA. For the acceptor groups, the strength is: −OMe < −CN < $-NO_2$. As the number of aromatic units in the initiator group increases from phenyl to perylene, the HOMO rises above and the LUMO drops below the energy levels of the F8 backbone of the molecular wire. Additionally, the HOMO and the LUMO levels become more spatially localized on the donor end group along that series. Consequently, the donor strength increases, which facilitates the CT process, but the driving force for ET also increases. Thus, if only ET (Figure 2c) is desired, one of the end groups should have both a high HOMO and a low LUMO energy with the frontier orbitals localized on that end group (the perylene moiety fulfills these requirements), while the other end group should be a poor donor and acceptor.

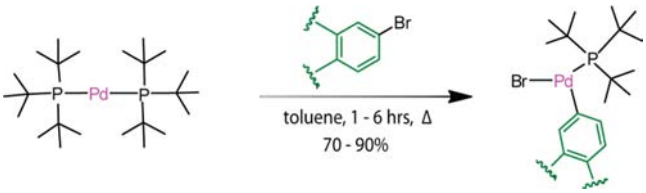


**Figure 3.** General one step synthetic procedure which was employed in order to synthesize the Pd (II) initiator complexes.

On the other hand, CT (Figure 2b) requires a donor end group that has both high-lying HOMO and LUMO energy levels and an acceptor end group with low-lying HOMO and LUMO energy levels as well as overall frontier orbitals that are fully spatially separated. Diphenylamine (DPA) paired with *p*-nitro-phenyl is a good candidate for this purpose; Figure 2e presents fully spatially separated frontier orbitals for the DPA−$(F2)_4$−$NO_2$ system (See Figure S1 for more details).

EWGs, such as *p*-nitro-phenyl (*p*-Ph−$NO_2$) and *p*-cyano-phenyl (*p*-Ph−CN) substituents, were identified as promising acceptor groups for molecular wire systems as they possess low-lying, well-localized LUMO energy levels. Furthermore, the DPA group contains a nitrogen heteroatom which, in contrast to the aromatic hydrocarbons, introduces a localized dipole moment and can help with direct stabilization of a positive charge.

**Initiator Synthesis.** Controlled Suzuki chain-growth polymerization requires Pd-based initiators formed by reacting the relevant aryl-bromo species with the starting palladium complex Pd(0)($t$Bu$_3$P)$_2$ under inert conditions (see SI for details). Oxidation addition (OA) leads to the formation of a tricoordinated Pd(II) initiator complex, which is very reactive on account of a vacant site on the metal center and the bulky electron-donating ligand ($t$Bu$_3$P). The OA step for all initiator groups was followed by $^1$H and $^{31}$P NMR to estimate the required reaction times for full conversion of Pd(0)($t$Bu$_3$P)$_2$ into the desired initiator complex (see Figure S3). It is interesting to note that every initiator group displayed a distinct kinetic; in general, for larger aromatic ring systems, in which the LUMO level is lower (see Figure S2 for HOMO/LUMO calculations for the different aryl-bromide species), the OA occurred faster in comparison to the smaller aryl species. The required reaction times in toluene at 70 °C for quantitative conversion of the equimolar aryl-bromide and Pd(0)($t$Bu$_3$P)$_2$ mixture into the Pd(II)-initiator complexes were 2−5 h for 3-perylene-, 2-anthracene-, 1-pyrene-, and phenyl-bromide, respectively. For DPA-fluorene bromide the reaction time was 9 h. It is worth noting that within the polymerization time (15 min polymerization) no significant differences in the initiator reactivity or the final polymer properties were observed.

**Monomer Synthesis, Chain-Growth Polymerization, and *in Situ* End Capping.** The use of asymmetric AB monobromo monoboronic-ester monomers is one of the requirements for Suzuki polymerization to proceed via a chain-growth mechanism.[17,18,20−22] The chain-growth polymerization is initiated when monomer (**1**) is added to the Pd initiator complex solution.[17] First, a transmetalation step takes place between the monomer and the $t$Bu$_3$PPd(X)Br palladium complex which bears the aromatic moiety X, followed by a reductive elimination step. Subsequently, intramolecular migration of the Pd species to the C−Br chain end and oxidative addition occurs, followed by insertion of the Pd species via oxidation addition, leaving the chain end ready for further reaction with a new monomer.[18,20−22] When the monoboronic-ester quencher (Y−$BO_2$−pinacole) is added, the reaction is terminated when a final transmetalation and reductive elimination step has occurred.

When the polymerization was carried out at 0 °C under inert conditions (see SI for polymerization details) employing different initiator groups (X) and quencher groups (Y), well-defined polymers with different properties were obtained. Most importantly, the polymer chains carried exactly one X and one Y end group, as confirmed by matrix-assisted laser desorption ionization time-of-flight (MALDI-TOF) mass spectrometry. Figure 4a−c depicts representative MALDI-TOF spectra of the DPA−pF8−CN polymers which show a narrow $M_w$ distribution and full functionalization of both chain ends. The presence of an initiator moiety and a quencher group on every polymer chain strongly supports the proposed chain-growth mechanism (under MALDI-TOF limitations). End group fidelity of >95% was measured by MALDI-TOF for most of the polymers, with the worst end group fidelities according to MALDI TOF still >86% in the case of Pyr−pF8−$NO_2$ (see SI for more details).

Likewise, THF gel permeation chromatography (GPC) measurements show narrow unimodal elution curves corresponding to polymers with a low PDI (1.20−1.40 for crude samples, see Table S1), corroborating the MALDI-TOF findings. $^1$H NMR spectra of the polymers show, in addition to the expected aromatic peaks of the pF8 polymer, small peaks


dx.doi.org/10.1021/ja3080677 | J. Am. Chem. Soc. 2012, 134, 17769−17777

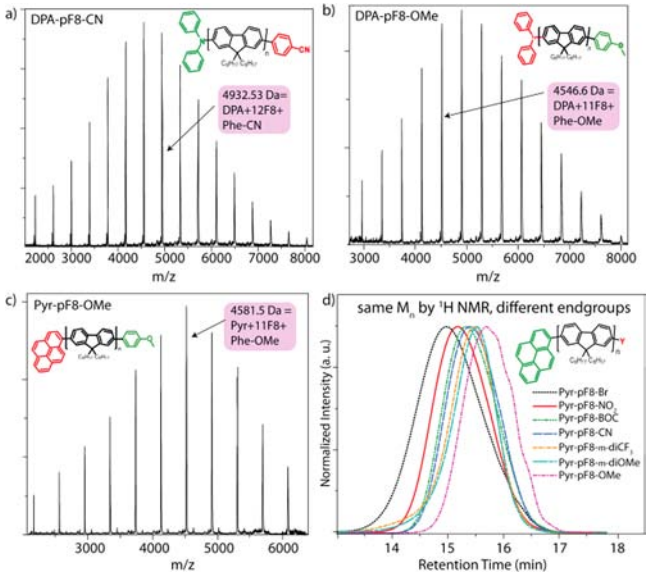


**Figure 4.** (a–c) Representative MALDI-TOF mass spectra for DPA–pF8–CN, DPA–pF8–MeO, and Pyr–pF8–MeO (see Figure S7 for other polymers). (d) THF–GPC profiles for Pyr–pF8–Y polymers, which have the same $M_n$ (as determined by $^1$H NMR) but different Y groups. GPC traces for the other X–pF8–Y synthesized polymers can be found in the SI.

in the aromatic regime which were attributed to the polymer end groups. In agreement with MALDI-TOF measurements, end group integration of a specific perylene aromatic proton versus the alkyl chain of pF8 in the $^1$H NMR of the Per–pF8–Br polymer (see Figures S8–S10 for more details) shows that degrees of polymerization (DP) of approximately 10–11 were obtained when monomer **1** was polymerized with 5 mol % of Pd initiator and quenched after 15 min. Extension of the polymerization time beyond 15 min yielded polymers with higher DP, however the success of end group incorporation decreases with higher monomer conversion, as was confirmed by MALDI TOF and $^1$H NMR. For example, after 30 min of polymerization, approximately 80% end capping was observed (DP of approximately 15). Decrease in end group fidelity with prolonged polymerization times was also reported for polyfluorene synthesis via Kumada chain-growth polymerization.[24] As the influence of end groups on the polymers photophysical properties is of key importance in this study, very high end group fidelity is necessary, and we therefore quenched the polymerizations with the required boronic esters at 50% conversion (15 min reaction time).

To demonstrate the controlled nature of the polymerization, the relationship between the conversion of monomer **1** and the different Pd initiators was investigated. Conversion–$M_n$ and conversion–PDI plots for the polymerization of **1** with 5 mol % of Pyr–Pd–($t$Bu$_3$P)Br, Per–Pd–($t$Bu$_3$P)Br, and DPA–Pd–($t$Bu$_3$P)Br revealed that the $M_n$ increases linearly in proportion to the conversion of the monomer while maintaining low PDI throughout the polymerization course (Figure 5). To follow the polymerization kinetics, aliquots were taken during the course of polymerization and analyzed by means of GPC and MALDI-TOF for initiations with Pyr–Pd–($t$Bu$_3$P)Br, Per–Pd–($t$Bu$_3$P)Br, and DPA–Pd–($t$Bu$_3$P)Br. As can be seen in Figures S4–S6, the unimodal elution curves are shifted toward higher $M_n$ over time, which is another typical feature of a chain-growth mechanism. Moreover, MALDI-TOF spectra (Figures

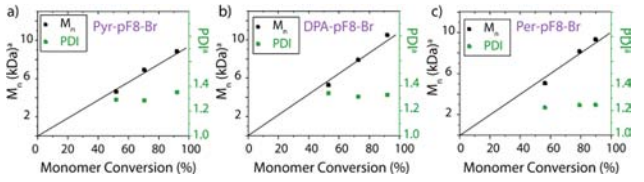


**Figure 5.** $M_n$ and $M_w/M_n$ (PDI) values of poly(9,9-dioctylfluorene) as a function of monomer conversion, obtained with monomer **1** and 5 mol % of (a) Pyr–Pd($t$Bu$_3$P)Br, (b)DPA–Pd($t$Bu$_3$P)Br, and (c) Per–Pd($t$Bu$_3$P)Br. Average values were calculated from MALDI-TOF measurements (see SI for further details), but PDI values were obtained from GPC.

S4–S6) also show that the polymer peaks shift to higher $M_n$ over the polymerization course. Additionally, all the polymer chains contain one initiator and one Br/H group on the other side. (Note: the Br/H is a typical group for polymerization which is quenched with acid, as was reported previously).[22,54] In summary, the linear conversion plots, the steady unimodal increase of $M_n$ with polymerization time, and the specific and defined end groups indicate that the polycondensation polymerization proceeded in a controlled fashion (chain-growth mechanism).

Finally, when the ratio between the Pd initiator and monomer **1** were varied, longer PMW were obtained, which increases potential use of this method. Figure 6 shows PMW

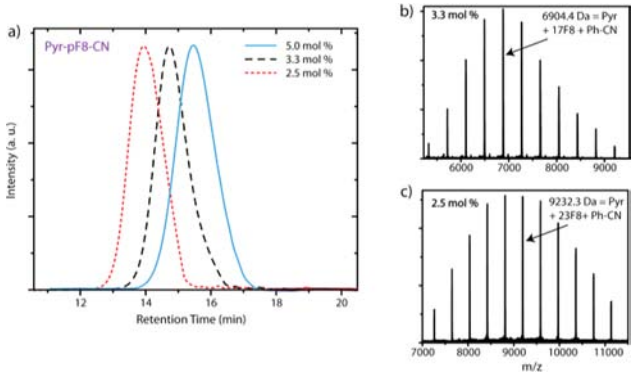


**Figure 6.** (a) GPC profiles of **1** with Pyr–Pd–($t$Bu$_3$P)Br obtained at initiator ratio of 5 mol % (solid blue), 3.3 mol % (dashed black), and 2.5 mol % (dotted red). The unimodal curves show a shift to lower retention time (which corresponds to higher $M_n$) when a lower feed ratio between the monomer and the initiator was used, while preserving low PDI (1.21–1.25). The GPC chromatograms were obtained after removing the monomer from the mixture (by precipitation with methanol). MALDI-TOF mass spectra of (b) 3.3 and (c) 2.5 mol %. For MALDI-TOF spectrum of 5 mol % please see Figure S7.

with higher $M_n$ and DPs of approximately 17 and 23 were synthesized with 3.3 and 2.5 mol % Pd initiator, respectively, while very high end group fidelity and low PDI (1.21–1.25) were preserved. It is important to note that in order to achieve high end group fidelity, the reactions were quenched with monoboronic-ester at approximately 50% conversion (see discussion above and SI for further details).

Interestingly, although all the polymers have a similar DP (determined by $^1$H NMR and MALDI-TOF), the elution times on the THF-GPC for the polymer series were remarkably different, as is presented in Figure 4d. This finding indicates that the properties of the X–pF8–Y polymers, i.e., interaction


dx.doi.org/10.1021/ja3080677 | J. Am. Chem. Soc. 2012, 134, 17769–17777

with the stationary phase of the column, were substantially modified through the incorporation of the end groups. See Figure S11 for the elution curves of all the polymers obtained from the GPC.

**Physical Characterization.** In order to examine whether the different polymers also show modified optoelectronic properties resulting from their different end groups, the optical properties were investigated by steady-state, transient absorption, and fluorescence spectroscopy. It is important to mention that all the polymers consist of on average 10−11 repeating units and have similar PDI (1.20−1.40). Thus the differences in the optoelectronic properties of these polymers do not stem from changes in the chain length and the PDI but rather from the interaction of the specific end groups with the pF8.

**Steady-State Absorption and Fluorescence Studies.** Only small changes are evident in the steady-state absorption spectra (0.01 mg/mL of polymer in anhydrous THF, rt) for most of the materials. However, in the series of X−pF8−$NO_2$ polymers, $\lambda_{max}$ is slightly red-shifted in comparison to the other X−pF8−Y spectra (see Figure S12 for all the absorption spectra). For example, $\lambda_{max}$ for Pyr−pF8−$NO_2$ (Figure 7a) is

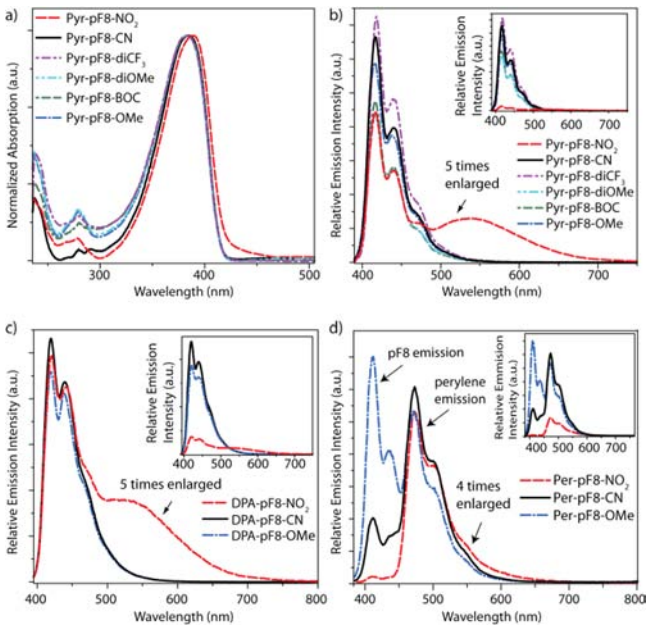


**Figure 7.** (a) Normalized optical absorption spectra of (0.01 mg/mL in THF at rt) Pyr−pF8−Y polymers. (b−d) Normalized PL spectra for Pyr−pF8−Y, DPA−pF8−Y, and Per−pF8−Y polymers, respectively. For Pyr/DPA−pF8−$NO_2$ and Per−pF8−$NO_2$ (red lines), the emission spectra are shown after scaling by 500 and 400%, respectively. The insets show the real ratios.

389 nm, and for the other Pyr−pF8−Y polymers it is 383 nm. This may imply that a weak CT state is formed, which is expected from the energy level alignment. On comparing the PL spectra, in anhydrous THF, of the different polymers, the presence of a CT state in X−pF8−$NO_2$ polymers (excluding the polymers with perylene end group) is further substantiated. Figure 7b,c shows representative normalized (by absorbance of sample at 388 nm) PL spectra for Pyr−pF8−$NO_2$ and DP−pF8−$NO_2$, respectively, where the polymers were irradiated at the pF8 absorption maximum, 388 nm. In detail, all the polymers have similarly shaped PL spectra, but for the X−pF8−$NO_2$ polymers a new, low-intensity, red-shifted, and broad band (around 550 nm) was detected. Similar features in the emission spectra are well documented for CT states of other materials in the literature.[55] Additionally, the pF8 emission (380−500 nm) is strongly quenched for the X−pF8−$NO_2$ polymers, which suggests that most of the pF8 excitons undergo some degree of charge separation to form CT states with the electron and hole density preferentially localized on the energetically more favorable chain ends. Moreover, since the emission from the pF8 bridge is almost completely quenched and the concentration of the solution is fairly low (0.01 mg/mL), it is very likely that intramolecular CT states are formed. The same trends were observed when the polymers were irradiated at 235 and 277 nm (see Figure S14 for further details). For the PL spectra of all synthesized polymers, please refer to Figure S13.

Figure 7d shows an absorption normalized PL spectrum where the HOMO/LUMO energy level alignment of X−pF8−Y was designed to be suitable for an ET process (Figure 2c). Specifically, when the Per−pF8−CN and Per−pF8−OMe polymers were irradiated at the pF8 absorption maximum (388 nm), intense perylene emission ($\lambda_{max}$ = 475 nm) was observed, which indicates that ET from pF8 to the perylene end group occurred. For Per−pF8−$NO_2$, both ET and CT were observed as indicated by the overall reduction in the emission intensity and the appearance of a broad red-shifted emission tail superimposed on the perylene emission.

**Solvent Effects.** Having established that charge separation can occur in the X−pF8−Y polymers as a function of the end groups in THF solution, we investigated the effect of the solvent environment on the emission properties of the polymers. The area-normalized fluorescence spectra of Pyr−pF8−$NO_2$, DPA−pF8−$NO_2$, and DPA−pF8−OMe were obtained in various solvents ranging from poor Lewis-donating solvents (hexane, DCM, chloroform; Gutmann donor number (DN) < 2) to good Lewis-donating solvents (acetonitrile, 1,4-dioxane, ethyl acetate, THF; DN > 10).

While the absorption spectra showed no significant differences, the emission spectra were found to be strongly dependent on both the solvent properties and the polymer end groups, as shown in Figure S15. Two main effects were observed: First, for X−pF8−$NO_2$, the broad red-shifted band (around 550 nm) was detected in good Lewis-donating solvents, while it was absent in the poor Lewis-donating solvents. As expected, no CT band was detected for DPA−pF8−OMe in any solvent. These findings are in line with the proposed CT state in the X−pF8−$NO_2$ polymers as Lewis-donating solvents can help to stabilize the positive charges through the involvement of their lone-pairs (the oxygen and nitrogen atoms in the solvents). Additionally, in agreement with a coordinating role of the solvent in CT stabilization, the CT emission band is more prominent in the rotationally restricted, cyclic ether solvents THF, and 1,4-dioxane than for the more flexible diethyl ether.

Second, the pF8 emission band (380−500 nm) is red-shifted and changes its shape with increasing solvent polarity [from apolar (hexane; dielectric constant ($\varepsilon_r$) = 1.9 to polar (acetonitrile; $\varepsilon_r$ = 37)]. This behavior is a typical sign of a general solvent effect, which is well-known for small molecule fluorophors with high dipole moment (push−pull systems).[56−59] Particularly large red-shifts and pronounced changes in the shape and intensity of the pF8 emission band were observed for the DPA−pF8−X polymers, resulting from the localized dipole moment caused by the DPA group. It should be also noted that no aggregation was observed (e.g., no


dx.doi.org/10.1021/ja3080677 | J. Am. Chem. Soc. 2012, 134, 17769−17777

Rayleigh-scattering in the fluorescence experiments was seen) for any of the aforementioned experiments, i.e., the spectral features are an inherent property of the polymeric chains and their interactions with the solvent environment.

It is important to mention that green emission (500−600 nm) is often observed in polyfluorene-based polymers in both polar and apolar solvents, originating from keto defects. Keto defects characterized by their n−$\pi^*$ transitions (400−500 nm) are also seen in the absorption spectrum.[60] In our study, the CT emission was only observed for X−pF8−$NO_2$ polymers dissolved in Lewis-donating solvents, as presented in Figure S15. Furthermore, no keto band was observed in the absorption spectra. Thus, the high wavelength emission of X−pF8−$NO_2$ polymers originates from a CT state and is not attributed to structural defects in the fluorene units.

We also investigated the contribution of the solvents in stabilization of the negative charge of the CT state on X−pF8−$NO_2$ polymers. Several literature reports have demonstrated that protonation of the CT excited states can occur in protic solvents.[59,61] A strong quenching in the intensity of the CT emission band was observed for the X−pF8−$NO_2$ polymers when a small amount (0.5 vol %) of methanol was added (Figure S16), which is a typical sign of a specific solvent effect. Protonation of the very electron-rich nitro-group of the X−pF8−$NO_2$ CT excited state by the protic solvent methanol is the likely cause of this effect (see Figure S16, inset). Additionally, such a small amount of methanol can neither cause significant changes in the overall refractive index nor in the static dielectric constant of the solvent, which explains why the pF8 emission band remains virtually unchanged when a low fraction of the protic cosolvent was added.

**Fluorescence Lifetime.** Time correlated single photon counting (TCSPC) was used to measure the PL decay at two wavelengths: 475 nm which predominantly arises from the radiative decay of the pF8 exciton and 580 nm which corresponds to emission from the CT state. CT states exhibiting red-shifted emission typically have longer lifetimes than excitonic states in the parent materials.[62,63] As shown in Figure 8, only when Y = $NO_2$ in DPA−pF8−Y polymers was CT emission detected at 580 nm with a longer lifetime ($\tau$ = 2.1 ns) than that of the pF8 exciton at 475 nm ($\tau$ = 0.6 ns) (Note that due to overlap of the pF8 exciton and CT state emission, the tail of the pF8 fluorescence is seen at 580 nm if no CT state emission is present.) Similar results were observed for Pyr−pF8−Y, see Figure S17 for details. In polymers designed for ET a characteristic decay time ($\tau$ = 2.1 ns) for the perylene emission is seen in both Per−pF8−Br and Per−pF8−$NO_2$ (see Figure S18). This suggests that once the exciton has transferred to the perylene, it remains there and is not influenced by the other end group.

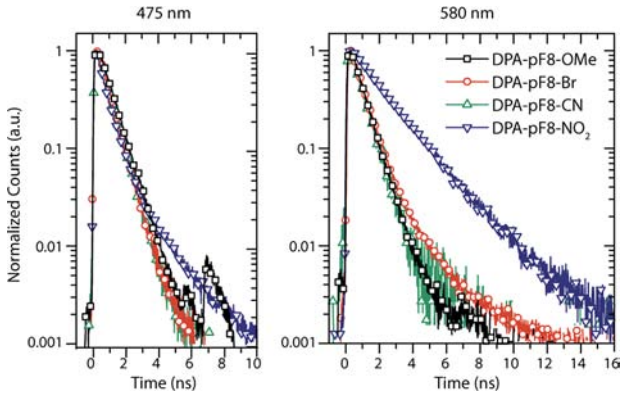


**Figure 8.** PL decay kinetics at selected wavelengths of 475 nm, corresponding to fluorescence from the pF8 exciton, and 580 nm, which is in the range of emission from the CT state, for the DPA−pF8−Y series of materials ($\lambda_{ex}$ = 407 nm, 0.01 mg/mL in anhydrous THF, rt).

**Transient Absorption Spectroscopy.** While emission spectroscopy indicates that a CT state is formed in certain X−pF8−Y polymers, other photophysical effects could potentially explain the observation of such new, red-shifted, and long-lived emission bands. Thus, transient absorption spectroscopy was employed to gain further insight. Transient absorption spectroscopy involves measuring the evolution of the differential transmission ($\Delta T/T$) of a sample over time, subsequent to an excitation pulse generating new photoexcited species. Increased transmission, positive $\Delta T/T$, is caused by either depopulation of the ground state, called ground-state bleach, or by stimulated emission of a photexcited species. Decreased transmission, negative $\Delta T/T$, arises from the photoinduced absorption (PIA) of excited-state species present. Nonemissive species can be probed using transient absorption spectroscopy, and the temporal behavior allows the population dynamics of photoexcited species to be studied.

The transient absorption spectra for Pyr−pF8−Y with a range of acceptor moieties at selected times of 1 ps and 1 ns after excitation is shown Figure 9a. The wavelengths probed do not cover the ground-state absorption so only photoinduced absorptions of excited-state species are observed, and the ground-state bleach is not. The initially created species (1 ps), with a PIA peaking at 750−800 nm, is the exciton on the pF8 chain, which is in good agreement with literature.[64] The temporal evolution of the differential transmission in the 750−800 nm region is shown in Figure 9c. From the monoexponential fit to the Pyr−pF8−OMe data, it can be seen that the pF8 exciton lifetime ($\tau$ = 0.56 ns) for Pyr−pF8−Y (Y = OMe, Br, CN) is in excellent agreement with that obtained by TCSPC (see Figure S19), further confirming the peak assignment. Only the pF8 exciton is observed for Pyr−pF8−Br, Pyr−pF8−OMe, and Pyr−pF8−CN.

In contrast, for Pyr−pF8−$NO_2$ the pF8 exciton species is rapidly quenched on the picosecond time scale, corresponding to the formation of a CT state. The significantly different feature peaked around 600 nm in the 1 ns spectra of Pyr−pF8−$NO_2$ is consistent with the formation of a CT state, and as shown by the kinetic trace averaged over 550−600 nm in Figure 9c, it is seen to grow in as the pF8 exciton decays, with the maximum population reached at ≈20 ps. The decay of this feature also matches well with that of the CT state luminescence as measured by TCSPC (see Figure S19).

The same trend in the decay of the pF8 exciton, i.e., faster decay for the $NO_2$ acceptor, can also be observed in the DPA−pF8−Y series, as shown with a comparison to the Pyr−pF8−Y series in Figure 9d. Similarly, a new feature is also seen in the transient absorption spectra as shown in Figure 9b. However, in the DPA donor series it must be concluded that there is also another process involved. Specifically, the lifetime of the pF8 excitation is lower for DPA−pF8−Y than for Pyr−pF8−Y (Y = Br, CN, OMe), hence, addition of the DPA end group is clearly depopulating the pF8 exciton species for these end groups, but not as efficiently and at a slower rate than the $NO_2$ acceptor end group. The depopulation of the pF8 exciton by DPA


dx.doi.org/10.1021/ja3080677 | J. Am. Chem. Soc. 2012, 134, 17769−17777

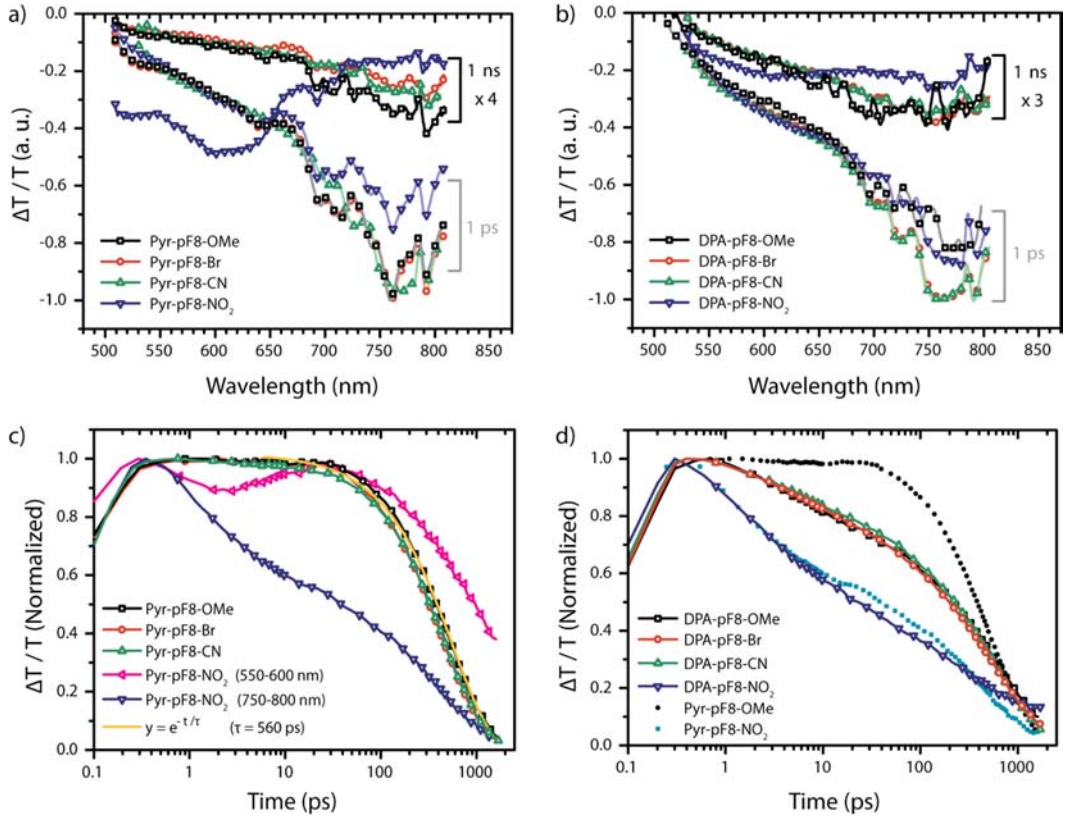


**Figure 9.** Transient absorption spectra of (a) Pyr−pF8−Y series and (b) DPA−pF8−Y series for a range of acceptor moieties, Y. The 1 ns spectra are scaled by a factor of 4 and 3, respectively, for increased clarity. The associated kinetic traces, averaged over the 750−800 nm range are shown for (c) the Pyr−pF8−Y series and (d) the DPA−pF8−Y series. The kinetic trace averaged over 550−600 nm is also included for Pyr−pF8−$NO_2$ in (c) ($\lambda_{ex}$ = 400 nm).

suggests a new species being formed, which is supported by the change in shape of the DPA−pF8−Y (Y = Br, CN, OMe) PIA over time (in contrast to the Pyr−pF8−Y materials which show negligible change, for comparison see Figure S20) and the nonexponential, multitime scale decay kinetic for the pF8 exciton in these polymers. In addition, the ground-state absorption spectrum of the DPA−pF8−Y polymers is similar to that of the Pyr−pF8−Y polymers, suggesting there is no significant change in the ground state. It must also be concluded that this species is nonemissive. The species formed when the DPA donor end group is present is postulated to have CT character.

The perylene donor polymers, Per−pF8−Y (Y = Br, $NO_2$), in which ET occurs were also studied using transient absorption spectroscopy. The results are consistent with ET to the perylene in both cases and for Per−pF8−$NO_2$ there is also competing CT state formation as was expected from the steady state fluorescence measurements. Details are included in the SI (Figure S21).

Bearing in mind that, for this study, the absorbing unit in these molecules is the fluorene chain chromophore(s) and CT/ET occurs from the bridge to the end groups, it is likely that CT proceeds *via* through-bond coupling while ET could be through-bond or through-space Förster resonance ET. From transient absorption spectroscopy, an estimated rate constant of $k > 10 \times 10^9$ $s^{-1}$ was obtained for both the CT in the X−pF8−$NO_2$ and the ET in the Per−pF8−Y polymers. Similar CT and ET rate constants were reported for fully conjugated molecular wires with much shorter bridges for which through-bond CT/ET mechanisms were proposed.[51,52] Surprisingly, in our system, preliminary studies show that both CT and ET emission bands have higher relative intensity for a bridge length of 10 as opposed to 5 repeating units (Figures S22 and S23, respectively), thus further investigation into the mechanism is needed to elucidate the CT/ET mechanism in the X−pF8−Y polymers.

## CONCLUSIONS

A fast, efficient and facile synthetic approach to obtain near quantitative heterobis-functionalized fully $\pi$-conjugated polymers *in situ* was presented. Since the end group functionality alters the optoelectronic properties of the fluorene bridge, this approach is a complementary route for molecular wire synthesis, and it has significant synthetic advantages over currently available multistep syntheses of small-molecule wires. We utilized Suzuki chain-growth polymerization of asymmetric fluorene (F8) monomers, showing typical features of controlled polymerizations such as control over MW, narrow PDI and the ability to independently introduce different end groups. A wide range of asymmetric, fully $\pi$-conjugated, well-defined X−pF8−Y structures were obtained with excellent end group fidelity and in high purity. End group fidelity was preserved for polymers with DPs up to 23 if the conversion was kept at around 50%.

In order to enable the resulting polymers to undergo either CT or ET processes, several end groups with different donor/acceptor nature were coupled to the polymer backbone. In agreement with predictions by DFT calculations, intramolecular, CT states with increased lifetime were formed in


dx.doi.org/10.1021/ja3080677 | J. Am. Chem. Soc. 2012, 134, 17769−17777

the nitro-terminated polymers, while efficient ET was observed for polymers initiated from perylene.

Since Suzuki reactions can proceed under mild reaction conditions and tolerate a wide range of monomers and functional groups, our methodology should be applicable to quick and facile synthesis of a large variety of well-defined PMW. Moreover, such materials will also allow for an in-depth systematic study of the influence of end groups on the chemical and optoelectronic properties of fully $\pi$-conjugated polymers.

## ■ ASSOCIATED CONTENT

### Supporting Information

Detailed experimental procedures of small molecules, palladium initiators, and polymers synthesis, their characterizations by MALDI-TOF, THF GPC, $^1$H, and 2D NMR, steady-state and transient absorption, and PL spectra as well as further DFT calculations can be found in the ESI. This material is available free of charge via the Internet at http://pubs.acs.org.

## ■ AUTHOR INFORMATION


### Corresponding Author

wtsh2@cam.ac.uk; w.huck@science.ru.nl


### Notes

The authors declare no competing financial interest.

## ■ ACKNOWLEDGMENTS

We are grateful for the financial support from the Engineering and Physical Sciences Research Council (ESPRC) (project EP/G060738/1) and Cambridge Display Technology (CDT) company. Likewise, E.E. thanks B'ani B'rith organization, and F.B. thanks the German Academic Exchange Service (DAAD) for financial aid. We thank Dr. Oren A. Scherman for helpful discussions.

## ■ REFERENCES


(1) Scherf, U.; Gutacker, A.; Koenen, N. *Acc. Chem. Res.* **2008**, *41*, 1086.

(2) Albini, A. *Photochemistry*; Royal Society of Chemistry: Cambridge, U.K., 2011; Vol. *39* (Specialist Periodical Reports).

(3) Sheina, E. E.; Liu, J. S.; Iovu, M. C.; Laird, D. W.; McCullough, R. D. *Macromolecules* **2004**, *37*, 3526.

(4) Miyakoshi, R.; Yokoyama, A.; Yokozawa, T. *J. Am. Chem. Soc.* **2005**, *127*, 17542.

(5) Javier, A. E.; Varshney, S. R.; McCullough, R. D. *Macromolecules* **2010**, *43*, 3233.

(6) Yokozawa, T.; Nanashima, Y.; Ohta, Y. *ACS Macro Lett.* **2012**, *1*, 862.

(7) Bronstein, H. A.; Luscombe, C. K. *J. Am. Chem. Soc.* **2009**, *131*, 12894.

(8) Lanni, E. L.; McNeil, A. J. *J. Am. Chem. Soc.* **2009**, *131*, 16573.

(9) Tkachov, R.; Senkovskyy, V.; Komber, H.; Sommer, J. U.; Kiriy, A. *J. Am. Chem. Soc.* **2010**, *132*, 7803.

(10) Ono, R. J.; Kang, S.; Bielawski, C. W. *Macromolecules* **2012**, *45*, 2321.

(11) Senkovskyy, V.; Tkachov, R.; Komber, H.; Sommer, M.; Heuken, M.; Voit, B.; Huck, W. T. S.; Kataev, V.; Petr, A.; Kiriy, A. *J. Am. Chem. Soc.* **2011**, *133*, 19966.

(12) Kohn, P.; Huettner, S.; Komber, H.; Senkovskyy, V.; Tkachov, R.; Kiriy, A.; Friend, R. H.; Steiner, U.; Huck, W. T. S.; Sommer, J. U.; Sommer, M. *J. Am. Chem. Soc.* **2012**, *134*, 4790.

(13) Miyakoshi, R.; Shimono, K.; Yokoyama, A.; Yokozawa, T. *J. Am. Chem. Soc.* **2006**, *128*, 16012.

(14) Huang, L.; Wu, S. P.; Qu, Y.; Geng, Y. H.; Wang, F. S. *Macromolecules* **2008**, *41*, 8944.

(15) Chujo, Y. *Conjugated Polymer Synthesis*; WILEY-VCH Verlag GmbH & Co. KGaA: Weinheim, Germany, 2010.

(16) Smeets, A.; Willot, P.; De Winter, J.; Gerbaux, P.; Verbiest, T.; Koeckelberghs, G. *Macromolecules* **2011**, *44*, 6017.

(17) Yokoyama, A.; Suzuki, H.; Kubota, Y.; Ohuchi, K.; Higashimura, H.; Yokozawa, T. *J. Am. Chem. Soc.* **2007**, *129*, 7236.

(18) Beryozkina, T.; Boyko, K.; Khanduyeva, N.; Senkovskyy, V.; Horecha, M.; Oertel, U.; Simon, F.; Stamm, M.; Kiriy, A. *Angew. Chem., Int. Ed.* **2009**, *48*, 2695.

(19) Zhang, H.-H.; Xing, C.-H.; Hu, Q.-S. *J. Am. Chem. Soc.* **2012**, *134*, 13156.

(20) Yokozawa, T.; Kohno, H.; Ohta, Y.; Yokoyama, A. *Macromolecules* **2010**, *43*, 7095.

(21) Yokozawa, T.; Suzuki, R.; Nojima, M.; Ohta, Y.; Yokoyama, A. *Macromol. Rapid Commun.* **2011**, *32*, 801.

(22) Elmalem, E.; Kiriy, A.; Huck, W. T. S. *Macromolecules* **2011**, *44*, 9057.

(23) Schmitt, C.; Nothofer, H. G.; Falcou, A.; Scherf, U. *Macromol. Rapid Commun.* **2001**, *22*, 624.

(24) Traina, C. A.; Bakus, R. C.; Bazan, G. C. *J. Am. Chem. Soc.* **2011**, *133*, 12600.

(25) Miteva, T.; Meisel, A.; Knoll, W.; Nothofer, H. G.; Scherf, U.; Muller, D. C.; Meerholz, K.; Yasuda, A.; Neher, D. *Adv. Mater.* **2001**, *13*, 565.

(26) Lee, J. K.; Ko, S.; Bao, Z. N. *Macromol. Rapid Commun.* **2012**, *33*, 938.

(27) Tsui, N. T.; Torun, L.; Pate, B. D.; Paraskos, A. J.; Swager, T. M.; Thomas, E. L. *Adv. Funct. Mater.* **2007**, *17*, 1595.

(28) Harriman, A.; Mallon, L.; Ziessel, R. *Chem.—Eur. J.* **2008**, *14*, 11461.

(29) James, D. K.; Tour, J. M. In *Molecular Wires: from Design to Properties*; Springer/Verlag: Berlin, Germany, 2005; Vol. *257*, p 33.

(30) Tsuda, A.; Osuka, A. *Science* **2001**, *293*, 79.

(31) Wagner, R. W.; Lindsey, J. S. *J. Am. Chem. Soc.* **1994**, *116*, 9759.

(32) Gray, H. B.; Winkler, J. R. *Proc. Natl. Acad. Sci. U.S.A.* **2005**, *102*, 3534.

(33) Choi, S. H.; Frisbie, C. D. *J. Am. Chem. Soc.* **2010**, *132*, 16191.

(34) Luo, L. A.; Choi, S. H.; Frisbie, C. D. *Chem. Mater.* **2011**, *23*, 631.

(35) Liddell, P. A.; Kuciauskas, D.; Sumida, J. P.; Nash, B.; Nguyen, D.; Moore, A. L.; Moore, T. A.; Gust, D. *J. Am. Chem. Soc.* **1997**, *119*, 1400.

(36) Anderson, H. L. *Chem. Commun.* **1999**, 2323.

(37) Eng, M. P.; Albinsson, B. *Angew. Chem., Int. Ed.* **2006**, *45*, 5626.

(38) Molina-Ontoria, A.; Wielopolski, M.; Gebhardt, J.; Gouloumis, A.; Clark, T.; Guldi, D. M.; Martin, N. *J. Am. Chem. Soc.* **2010**, *133*, 2370.

(39) Cacialli, F.; Wilson, J. S.; Michels, J. J.; Daniel, C.; Silva, C.; Friend, R. H.; Severin, N.; Samori, P.; Rabe, J. P.; O'Connell, M. J.; Taylor, P. N.; Anderson, H. L. *Nat. Mater.* **2002**, *1*, 160.

(40) Weiss, E. A.; Ahrens, M. J.; Sinks, L. E.; Gusev, A. V.; Ratner, M. A.; Wasielewski, M. R. *J. Am. Chem. Soc.* **2004**, *126*, 5577.

(41) Wang, C. S.; Palsson, L. O.; Batsanov, A. S.; Bryce, M. R. *J. Am. Chem. Soc.* **2006**, *128*, 3789.

(42) Natera, J.; Otero, L.; D'Eramo, F.; Sereno, L.; Fungo, F.; Wang, N. S.; Tsai, Y. M.; Wong, K. T. *Macromolecules* **2009**, *42*, 626.

(43) Giacalone, F.; Segura, J. L.; Martin, N.; Ramey, J.; Guldi, D. M. *Chem.—Eur. J.* **2005**, *11*, 4819.

(44) Kurita, T.; Nishimori, Y.; Toshimitsu, F.; Muratsugu, S.; Kume, S.; Nishihara, H. *J. Am. Chem. Soc.* **2010**, *132*, 4524.

(45) Ashwell, G. J.; Urasinska-Wojcik, B.; Phillips, L. J. *Angew. Chem., Int. Ed.* **2010**, *49*, 3508.

(46) Bumm, L. A.; Arnold, J. J.; Cygan, M. T.; Dunbar, T. D.; Burgin, T. P.; Jones, L.; Allara, D. L.; Tour, J. M.; Weiss, P. S. *Science* **1996**, *271*, 1705.

(47) Davis, W. B.; Svec, W. A.; Ratner, M. A.; Wasielewski, M. R. *Nature* **1998**, *396*, 60.

(48) Nitzan, A.; Ratner, M. A. *Science* **2003**, *300*, 1384.

(49) Becker, K.; Lupton, J. M. *J. Am. Chem. Soc.* **2006**, *128*, 6468.

(50) Koenen, J. M.; Jung, S.; Patra, A.; Helfer, A.; Scherf, U. *Adv. Mater.* **2012**, *24*, 681.
(51) Harriman, A.; Mallon, L. J.; Elliot, K. J.; Haefele, A.; Ulrich, G.; Ziessel, R. *J. Am. Chem. Soc.* **2009**, *131*, 13375.
(52) Goldsmith, R. H.; Sinks, L. E.; Kelley, R. F.; Betzen, L. J.; Liu, W.; Weiss, E. A.; Ratner, M. A.; Wasielewski, M. R. *Proc. Natl. Acad. Sci. U.S.A.* **2005**, *102*, 3540.
(53) Miura, T.; Carmieli, R.; Wasielewski, M. R. *J. Phys. Chem. A* **2010**, *114*, 5769.
(54) Yokoyama, A.; Yokozawa, T. *Macromolecules* **2007**, *40*, 4093.
(55) Bredas, J. L.; Beljonne, D.; Coropceanu, V.; Cornil, J. *Chem. Rev.* **2004**, *104*, 4971.
(56) Lippert, E. *Z. Elektrochem.* **1957**, *61*, 962.
(57) Viard, M.; Gallay, J.; Vincent, M.; Meyer, O.; Robert, B.; Paternostre, M. *Biophys. J.* **1997**, *73*, 2221.
(58) Fitilis, I.; Fakis, M.; Polyzos, I.; Giannetas, V.; Persephonis, P.; Vellis, P.; Mikroyannidis, J. *Chem. Phys. Lett.* **2007**, *447*, 300.
(59) Lakowicz, J. R. *Principles of Fluorescence Spectroscopy*, 3rd ed.; Springer Science: New York, 2010.
(60) Chi, C. Y.; Im, C.; Enkelmann, V.; Ziegler, A.; Lieser, G.; Wegner, G. *Chem.—Eur. J.* **2005**, *11*, 6833.
(61) Tolbert, L. M.; Solntsev, K. M. *Acc. Chem. Res.* **2002**, *35*, 19.
(62) Morteani, A. C.; Friend, R. H.; Silva, C. *J. Chem. Phys.* **2005**, *122*, 244906.
(63) Petrozza, A.; Laquai, F.; Howard, I. A.; Kim, J. S.; Friend, R. H. *Phys. Rev. B* **2010**, *81*, 205421.
(64) Clark, J.; Nelson, T.; Tretiak, S.; Cirmi, G.; Lanzani, G. *Nat. Phys.* **2012**, *8*, 225.